ACTA MECHATRONICA

2022 Volume 7 Issue 1

International Scientific Journal about Mechatronics

electronic journal
ISSN 2453-7306

CONTENTS

(MARCH 2022)

Acta Mechatronica - International Scientific Journal about Mechatronics
Volume: 7 2022 Issue: 1 Pages: 1-7 ISSN 2453-7306

doi:10.22306/am.v7i1.82

Received: 03 Feb. 2022
Revised: 18 Feb. 2022
Accepted: 02 Mar. 2022

Kinematic motion analysis of the members of a double jaw crusher

Darina Hroncova
Department of Mechatronics, Faculty of Mechanical Engineering, Technical University of Košice, Park Komenského 8, 042 00 Košice, Slovak Republic, EU, darina.hroncova@tuke.sk (corresponding author)
Ingrid Delyova
Department of Applied Mechanics and Mechanical Engineering, Faculty of Mechanical Engineering, Technical University of Košice, Letná 9, 042 00 Košice, Slovak Republic, EU, ingrid.delyova@tuke.sk
Peter Frankovsky
Department of Applied Mechanics and Mechanical Engineering, Faculty of Mechanical Engineering, Technical University of Košice, Letná 9, 042 00 Košice, Slovak Republic, EU, peter.frankovsky@tuke.sk
Vojtech Neumann
Department of Applied Mechanics and Mechanical Engineering, Faculty of Mechanical Engineering, Technical University of Košice, Letná 9, 042 00 Košice, 042 00 Košice, Slovak Republic, EU, peter.frankovsky@tuke.sk
Dalibor Cech
Department of Applied Mechanics and Mechanical Engineering, Faculty of Mechanical Engineering, Technical University of Košice, Park Komenského 8, 042 00 Košice, Slovak Republic, EU, dalibor.cech@tuke.sk

Keywords: kinematic analysis, mechanism, simultaneous motion, simulation.

Abstract: Computational technology makes it possible to accelerate and simplify the processes of kinematic and dynamic analysis. The paper deals with the problem of kinematic analysis of a planar six-joint mechanism of a jaw double-spring crusher. Computational techniques and software support have been used in the kinematic analysis. The obtained results are compared with the results of the graphical solution. The graphical solution has been carried out by using CAD software. MSC.Adams/View program was used to create a model and simulate the jaw crusher motion. In both cases there was agreement of the obtained results.

1 Introduction

The development of computer technology has made it possible to simplify and speed up various processes in different industries. One of these industries is engineering. Computing is nowadays quite used in this field, it can be said that almost in the whole process of design, construction and production of a machine component, mechanism and others. The software that has been developed to facilitate the work of people in technical practice allows a given machine part to be designed as a 3D model, to combine multiple parts into an assembly to create a functional 3D model of, for example, a mechanism, to perform static, kinematic or dynamic analyses of parts, mechanisms, they also allow to plot the stresses of the parts, to simulate not only the processes of designing the parts, but also the simulation of the production of these parts. Last but not least, they save time and money because the designs can be carried out much faster compared to analytical methods, they also save the consumption of materials because they can simulate a number of things and processes in which it is possible to detect possible defects and shortcomings of a given component, mechanical system or manufacturing process before the prototype is made or production is started [1-3].

The aim of this thesis is to model the mechanism of a crusher with two struts in the MSC.Adams program environment, and then also to perform a kinematic analysis of the mechanism in this program.

2 Kinematic analysis of a double-spring crusher

The double jaw crusher is designed for crushing hard materials, also quarried materials, sand and gravel, and recycling. [4,5]

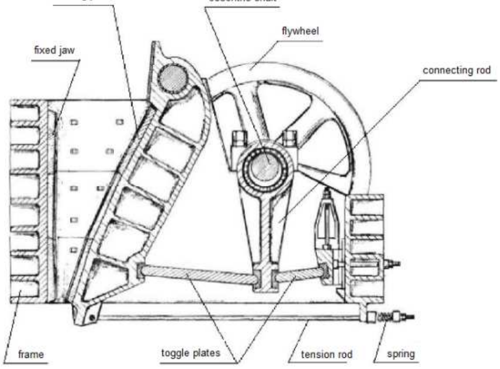

Figure 1 Description of the main parts of the double jaw crusher[4]

The tie rod and compression spring ensure that the buckling plates are in their bearings throughout the crusher run, and also assist in the reciprocating movement of the moving jaw. The kinematic analysis will be carried out on a simplified model of the crusher, where the rod and spring are neglected and the buckling plate fits are replaced by pivot joints. A simplified model (kinematic diagram) of the mechanism of the double buckling jaw crusher is shown in Fig. 20. The mechanism in question is a six membered mechanism formed by attaching a binary system group, composed of members 5 and 6, to a basic four membered crank mechanism composed of members 1, 2, 3 and 4. The members of this mechanism are a frame (1), an eccentric shaft, i.e. a crank (2), a connecting rod (3), a buckling plate, i.e. as it were a rocker arm (4), a second buckling plate (5) and a movable jaw with a pendulum (6) [4,5].

Member 2 is the driving member, the others are driven [6].

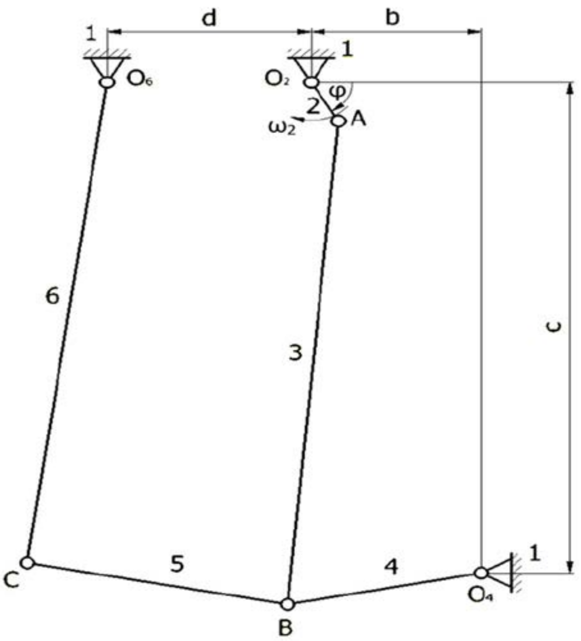

Figure 2 Kinematic diagram of the solved model - crusher mechanism

Every single moving member performs a planar motion, as it is a planar mechanism. Member 2 performs a uniform rotational motion about point O_2 with a constant angular velocity $\omega_2 = 6\pi\, rad/s$, the trajectory of point A is a circle. Members 4 and 6 also perform rotational motion, member 4 about point O_4 and member 6 about point O_6. The trajectories of points B and C are parts of a circle, namely circular arcs. Members 3 and 5 perform general planar motion. All these motions are related to the base space - the frame [6].

The dimensions of the individual members and the distances of the axes of rotation are: member 2 $O_2A = 40\, mm$, member 3 $AB = 430\, mm$, member 4 $O_4B = 145\, mm$, member 5 $BC = 195\, mm$, member 6 $O_6C = 430\, mm$, $b = 125\, mm$, $c = 435\, mm$, $d = 150\, mm$, uhol $\varphi = 60°$.

2.1 *Determining the velocity of individual members*

In the simultaneous motion of bodies, the resultant velocity of a given point or body consists of the drift velocity and the relative velocity, which can be determined graphically as a diagonal in a parallelogram, the sides of which are the vectors of the given velocity components. To determine the resultant velocity vector ($\boldsymbol{v}_v$), the vector summation relation of the drift velocity vector ($\boldsymbol{v}_u$) and the relative velocity vector ($\boldsymbol{v}_r$) holds [7]:

$$\boldsymbol{v}_v = \boldsymbol{v}_u + \boldsymbol{v}_r. \tag{1}$$

The magnitude of the velocity at point A can be determined by calculation at a known angular velocity.

$$v_{A21} = \omega_2 \overline{O_2A} = 0.75398\, m/s \tag{2}$$

When the motion of the members is decomposed, the velocity at point A is expressed by the equation.

$$\boldsymbol{v}_{A31} = \boldsymbol{v}_{A32} + \boldsymbol{v}_{A21} \tag{3}$$

Since point A is the common point of member 2 and member 3, the magnitude of the velocity $\boldsymbol{v}_{A32}$ is zero. Therefore, the velocity of point A is.

$$\boldsymbol{v}_{A31} = \boldsymbol{v}_{A21} = \boldsymbol{v}_A \tag{4}$$

Point B is a common point of Article 3 and Article 4 (also member 5). Thus, the magnitude of the velocity $\boldsymbol{v}_{B34}$ is zero. For the velocity at point B, with the decomposition of the motion $31 = 34 + 41$, the following is true.

$$\boldsymbol{v}_{B31} = \boldsymbol{v}_{B41} = \boldsymbol{v}_B \tag{5}$$

The velocity at point B can be determined graphically using the instantaneous centre of rotation of member 3 and the velocity at point A using the angle of view theorem. According to the decomposition of the motion, the vector equation holds for the velocity at point B.

$$\boldsymbol{v}_{B31} = \boldsymbol{v}_{A31} + \boldsymbol{v}_{BA31} \tag{6}$$

With respect to the reference point A, point B performs a planar rotational motion on a circle.

2.2 *Determining the accelerations of individual members*

Acceleration is generally a vector quantity that characterizes the temporal change in velocity of a point or body. When bodies move simultaneously, the resultant acceleration of a body or point is determined as the vector sum of the vector of the acceleration vector of the drift motion, the acceleration vector of the relative motion, and the Coriolis acceleration [7].

$$\boldsymbol{a}_v = \boldsymbol{a}_u + \boldsymbol{a}_r + \boldsymbol{a}_{cor}. \tag{7}$$

For the Coriolis acceleration $\boldsymbol{a}_{cor}$, relation (8) is generally valid; it is the vector product of twice the angular velocity vector of the drift motion ($\boldsymbol{\omega}_u$) and the velocity vector of the relative motion ($\boldsymbol{v}_r$) [1].

$$\boldsymbol{a}_{cor} = 2\boldsymbol{\omega}_u \times \boldsymbol{v}_r \tag{8}$$

The Coriolis acceleration is equal to zero when the translational drift is zero ($\boldsymbol{\omega}_u = 0$), or when the relative velocity at a given point is zero ($\boldsymbol{v}_r = 0$), or the vectors of these velocities are parallel at that point. When bodies are moving simultaneously in a plane, these vectors are perpendicular to each other, and thus the magnitude of the Coriolis acceleration is [7].

$$a_C = 2\omega_u v_r \tag{9}$$

Point A is the common point of members 2 and 3, and hence the acceleration at this point is also.

$$\boldsymbol{a}_{A31} = \boldsymbol{a}_{A21} = \boldsymbol{a}_A \tag{10}$$

Since member 2 rotates with a constant angular velocity ω_2, which results in a constant velocity v_A of point A, the acceleration of point A in the tangential direction is zero ($\boldsymbol{a}_{A21t} = 0\ ms^{-2}$). The acceleration at point A is equal to the normal component of the acceleration.

$$\boldsymbol{a}_{A21} = \boldsymbol{a}_{A21n} + \boldsymbol{a}_{A21t} \tag{11}$$

$$\boldsymbol{a}_{A21} = \boldsymbol{a}_{A21n} \tag{12}$$

The magnitude of the normal component of acceleration at a given point can be obtained using Euclidean construction.

It is known that point B is a common point of members 3 and 4 (and also of member 5), therefore.

$$\boldsymbol{a}_{B31} = \boldsymbol{a}_{B41} = \boldsymbol{a}_{B51} = \boldsymbol{a}_B \tag{13}$$

The acceleration at point B will.

$$\boldsymbol{a}_{B31} = \boldsymbol{a}_{A31} + \boldsymbol{a}_{BA31} \tag{14}$$

After decomposing the accelerations into tangential and normal components, relation (14) can be written in the form.

$$\boldsymbol{a}_{B31} = \boldsymbol{a}_{A31n} + \boldsymbol{a}_{A31t} + \boldsymbol{a}_{BA31n} + \boldsymbol{a}_{BA31t} \tag{15}$$

From the solution of the acceleration at point A, it is known that the magnitude of the tangential component of the acceleration $\boldsymbol{a}_{A31t}$ at point A is equal to zero, and the normal component of this acceleration $\boldsymbol{a}_{A31n}$ is also known, the acceleration $\boldsymbol{a}_{A31}$ is known completely. The other accelerations in relation (15) are unknown and need to be determined. The individual magnitudes of the components of the accelerations of point B with respect to the overlap and of point B with respect to point A have been determined graphically and their values are given in Table 1.

Point C is the common point of members 5 and 6, therefore.

$$\boldsymbol{a}_{C51} = \boldsymbol{a}_{C61} = \boldsymbol{a}_C \tag{16}$$

For the acceleration at point C, the relation.

$$\boldsymbol{a}_{C51} = \boldsymbol{a}_{B51} + \boldsymbol{a}_{CB51} \tag{17}$$

The acceleration at point B is completely known from relation (15) and therefore will not be decomposed into normal and tangential components. The other accelerations have to be found out. Relation (17), after decomposition into components, has the form.

$$\boldsymbol{a}_{C51} = \boldsymbol{a}_{B51n} + \boldsymbol{a}_{B51t} + \boldsymbol{a}_{CB51n} + \boldsymbol{a}_{CB51t} \tag{18}$$

The magnitude of the normal components of the accelerations ($\boldsymbol{a}_{C51n}$ a $\boldsymbol{a}_{CB51n}$) can be determined using the Euclidean construction of the given accelerations; the magnitudes of the tangential components of the accelerations ($\boldsymbol{a}_{C51t}$ a $\boldsymbol{a}_{CB51t}$) are determined from the vector pattern.

The actual magnitudes of the given acceleration velocities obtained by the graphical solution are given in Table 1. The graphical solution has been carried out in a CAD program.

Table 1. Velocities and accelerations obtained by graphical solution

	point				
	A	BA	B	CB	C
a_n [ms^{-2}]	14.2122	1.2828	1.3956	0.9306	0.0668
a_t [ms^{-2}]	0	5.8632	13.0544	12.6994	2.6872
a [ms^{-2}]	14.2122	6.002	13.1286	12.7334	2.6882
v [ms^{-1}]	0.75398	0.7427	0.44984	0.42598	0.16946

3 Motion simulation of the mechanism

The program allows to perform kinematic and dynamic analyses of mechanical systems of points or bodies, both rigid and flexible, as well as analyses of the strength of structural elements, sensing of forces in motion with consideration of gravitational, inertial effects or frictional forces, etc. The software also offers the possibility to model a given mechanical system directly in its own environment using the CAD functions it offers, or this model of the mechanism, mechanical system can be imported from various CAD software (e.g. from software such as Inventor, SolidWorks and others) in .sat, .step, .iam and other formats [8-12].

3.1 Model creation

The simulation was performed in MSC.Adams/View [13,14]. In this program, the individual members of the mechanism were successively modelled according to the simplified scheme in Fig. 2. The modelling function "RigidBody:Link" was used to create the individual members. When modelling the crank, the rotation point O_2 is placed in the position (0, 0, 0) mm and the length is defined according to the given dimensions. The crank is rotated in a position 60° from the x-axis. This is done by rotating the end markers by an angle of (300, 0, 0, 0)°, due to the fact that the angle of rotation about the z-axis is measured counterclockwise from the x-axis in the program. The buckling plate (member 4) is positioned so that its rotation point O_4 is at the position (125, -435, 0) mm. The connecting rod is attached to the pre-existing crank 2. The jaw has a pivot point at point O_6 with coordinates (-150, 0, 0) mm. A second buckling plate (member 5) is attached to this jaw. A model of the crusher mechanism is shown in Fig. 3.

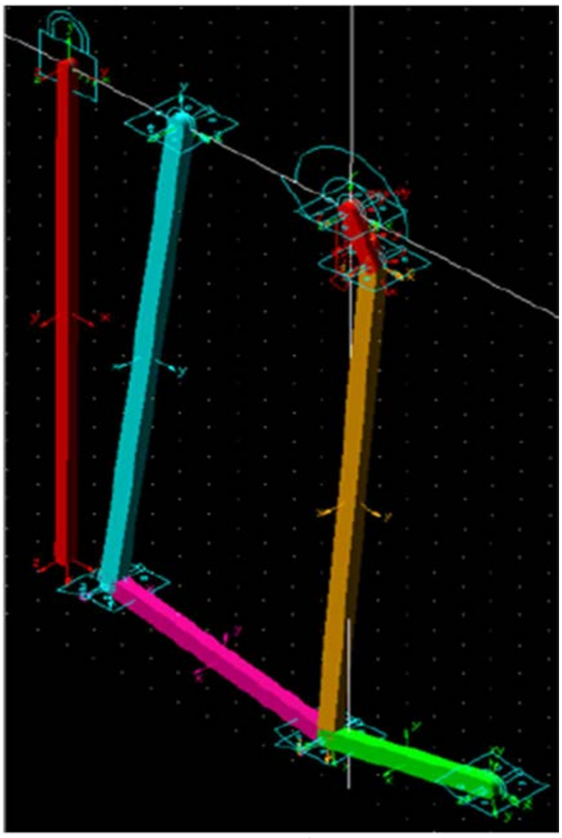

Figure 3 Kinematic model of the crusher mechanism

The individual members of the mechanism are connected by rotary linkages. After the model is assembled, the model is subjected to verification.

The driving member 2 (eccentric shaft) performs a rotary motion and rotates at an angular velocity of $\omega_2 = 6\pi\ rad/s$, which when converted to degrees per second is $\omega_2 = 1080\ °/s$. The crank makes 3 rotations in 1 second. The rotational motion is placed at the crank turning point O_2. The simulation is set so that the crank makes one revolution (360° rotation), and thus the simulation time is one-third of a second. The step size is set to 0.001.

In order to be able to obtain individual data of the monitored quantities during the movement of the mechanism, their meters were defined in the program, such as speed meter, acceleration meter, etc... In addition to the measurement of speed and acceleration, the angles of rotation of some members were also measured. The obtained results were processed in the postprocessor, in the form of graphs and tables.

3.2 Simulation results of selected variables

The simulation is run from an initial position where the driving member 2 is rotated by an angle $\varphi = 60°$ below the x-axis. This is in order to be able to compare the values obtained for the individual variables from the computer simulation with the values obtained by the graphical solution. The advantage of the simulation is that it offers the waveforms of the given quantities also depending on the movement of the driving member, i.e. during the action of the mechanism cycle.

Figure 4 shows the time history of the angle of the member 2. Figure 5 shows the waveform of the dependence of the angle of member 6 on the rotation of member 2 when the crank is turned one revolution. The angle of the movable jaw is measured from the x-axis.

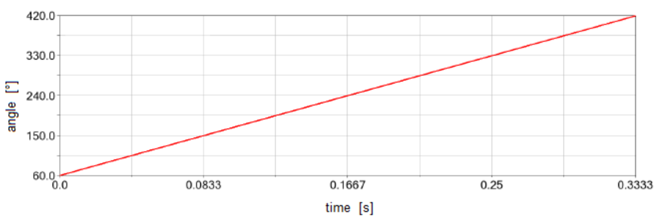

Figure 4 Time history of crank angle (member 2)

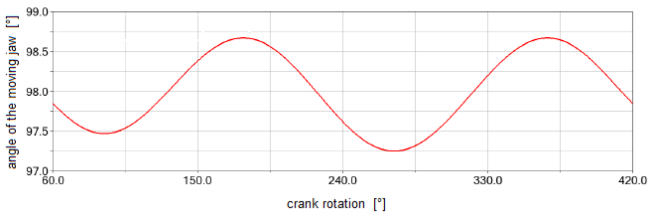

Figure 5 Course of the angle of the movable jaw (member 6) as a function of the rotation of the crank (member 2)

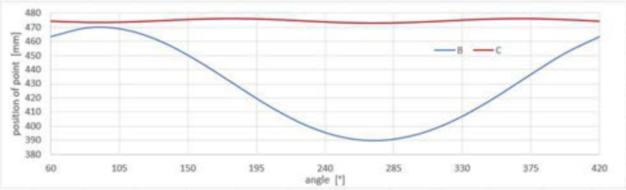

Figure 6 Dependence of the position of a point on the angle of rotation of the member 2

Figure 6 shows the dependence of the position of points B and C on the angle of rotation of the crank by one turn. From Figure 6, it can be seen that at one turn of the crank, the movable jaw approaches the fixed jaw twice. The first advancement of the movable jaw from the fixed jaw is less than the second advancement. The values at the moment when the movable jaw is closest to the fixed jaw are the same in both cases.

For the magnitude of the individual resulting accelerations at the given points, it is valid that they are equal to the square root of the sum of the squares of the components of the given acceleration.

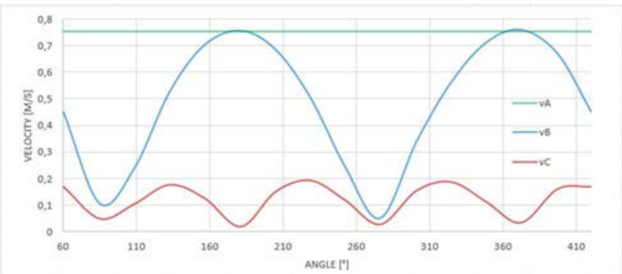

Figure 7 Velocity magnitude of single points as a function of member rotation angle 2

Figure 7 shows the evolution of the velocity of the individual points of the mechanism as a function of the angle of rotation of the crank when the crank is turned one revolution. Figure 8 shows the waveform of the acceleration components of point B as a function of the crank rotation. The resulting acceleration curves of the individual points of the mechanism as a function of crank rotation are shown in Figure 9.

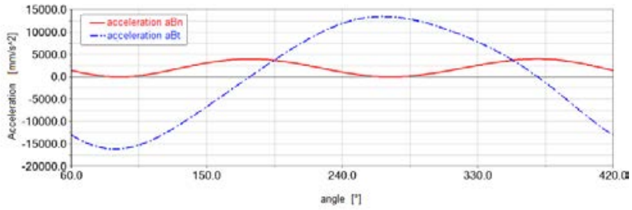

Figure 8 Acceleration components at point B as a function of crank rotation

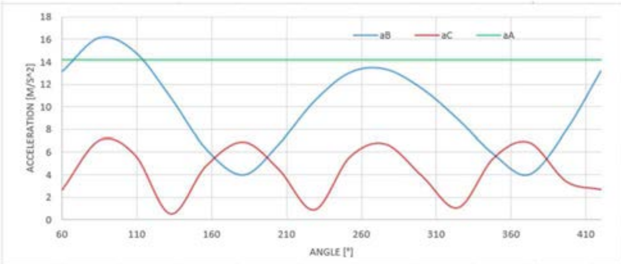

Figure 9 Acceleration of single points as a function of the angle of rotation of the member 2

3.3 Point trajectory

The advantage of the program and the simulation itself is that it can also provide a representation of the paths of given points. The trajectories of points A, B and C are shown using the "Trace Marker" function in Figure 10. The trajectory of point A is a circle, the trajectories of points B and C are circular arcs.

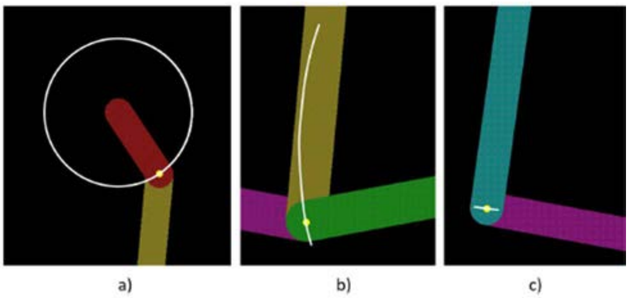

Figure 10 Trajectory of (a) point A, (b) point B, (c) point C

Another way to plot the path or trajectory of a given point during the movement of the mechanism is to plot it in the postprocessor as the dependence of the x-axis position of the component point on the y-axis component of the y-axis position. The individual point trajectories are shown in Figure 11.

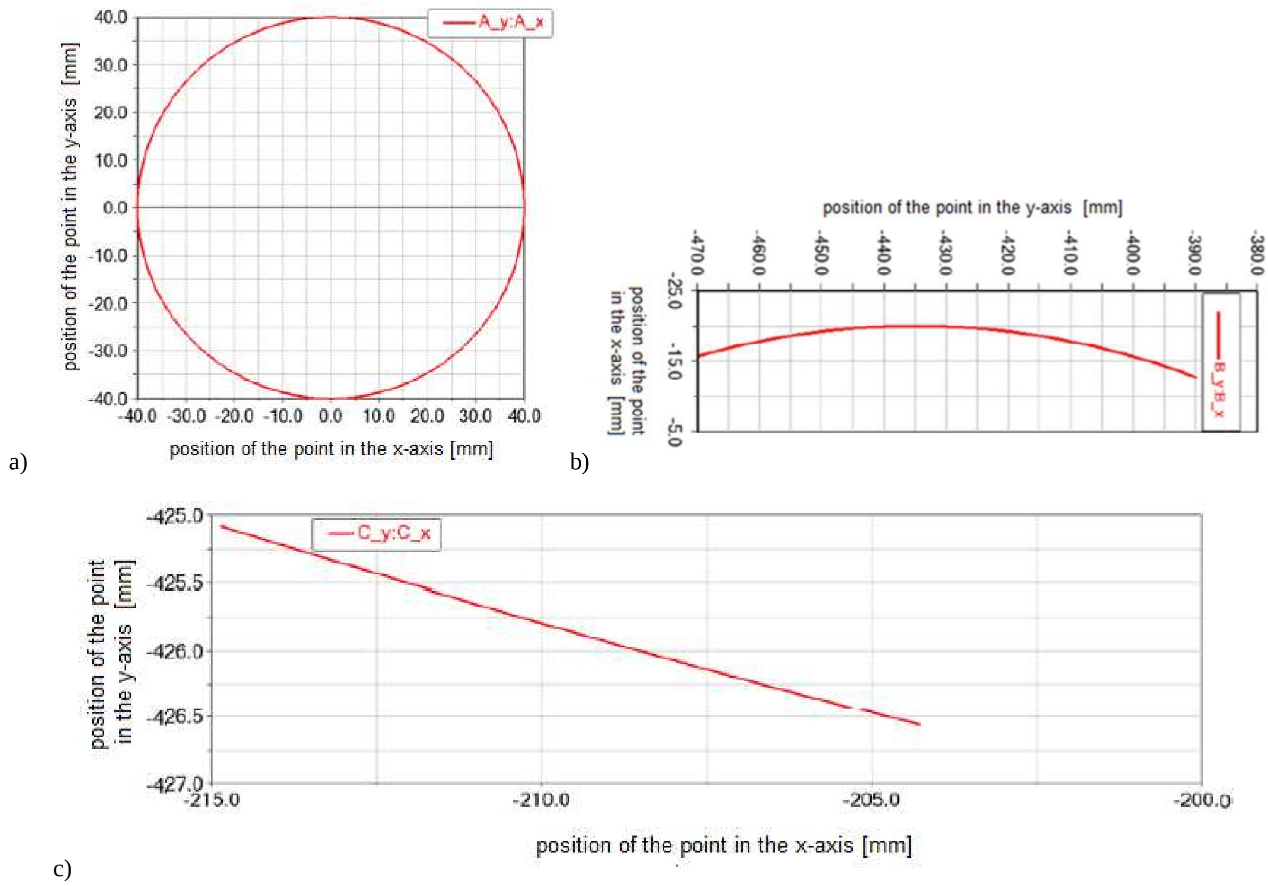

Figure 11 Trajectory of (a) point A, (b) point B, (c) point C

3.4 Comparison of results obtained by graphical solution and simulation

The displacements obtained by graphical solution and simulation were compared in the initial position of the mechanism. The individual deviations of the solutions are shown in Table 2. The largest differences in the results are visible only at the ten-thousandths place.

Table 2 Comparison of results obtained by graphical solution and simulation

	Graphic solution	Computer simulation	Difference
v_A [ms^{-1}]	0,75398	0,75398	0,00000
v_B [ms^{-1}]	0,44984	0,44984	0,00000
v_C [ms^{-1}]	0,16946	0,16946	0,00000
a_A [ms^{-2}]	14.21220	14.21223	0,00003
a_B [ms^{-2}]	13,12860	13,12876	0,00016
a_C [ms^{-2}]	2,68820	2,68813	-0,00007
a_{BA} [ms^{-2}]	6,00200	6,00200	0,00000
a_{CB} [ms^{-2}]	12,73340	12,73346	0,00006

4 Conclusion

In this paper, the kinematic analysis of the planar six-joint mechanism of a two-spring jaw crusher has been carried out. The kinematic analysis of the mechanism was solved graphically and by computer simulation.

The graphical solution was carried out using Autodesk Inventor Professional 2020 with the mechanism in the initial position. Kinematic analysis using computer simulation was solved using MSC.Adams/View program, where the waveforms and magnitudes of the given quantities during one complete cycle of the mechanism and the trajectories of the given points were obtained.

Based on the comparison of the results obtained by the two solution methods, it can be stated that the accuracy of the results obtained from the simulation is quite high compared to the graphical solution. One can speak of very small to imperceptible differences in the results, since the largest differences in the results found are in the order of 10^{-4} to 10^{-5} units.

Thus, the use of computer simulation of the mechanism is a suitable and advantageous choice for kinematic analysis, also because it provides results not only at a single instant, as in the graphical solution, but during the whole process or cycle. The given results can be processed in the form of graphs or even tables, and the simulation also provides an insight into how the mechanism will perform the prescribed motion.

Acknowledgements

This work was supported by the Ministry of Education of Slovakia Foundation under Grant project, VEGA No. 1/0436/22, VEGA No. 1/0500/20 and KEGA No. 027TUKE–4/2020.

[1] VAVRO jr, J., VAVRO, J., KOVÁČIKOVÁ, P., BEZDEDOVÁ, R., HÍREŠ, J.: Kinematic and dynamic analysis and distribution of stress in items of planar mechanisms by means of the MSC ADAMS software, *Manufacturing technology*, Vol. 17, No. 2, pp. 267-270, 2017.

[2] RATIU, M., RUS, A., BALAS, M.L.: *Modeling in ADAMS of a 6R industrial robot*, MATEC Web of Conferences, Vol. 184, pp. 1-4, 2018.

[3] HRONCOVÁ, D., DELYOVÁ, I., FRANKOVSKÝ, P.: *Kinematic analysis of mechanisms using MSC Adams*, Applied Mechanics and Materials, Trans Tech Publications Ltd, pp. 83-89, 2014.

[4] KOCHANOWSKY, B.: Portable crusher for open pit and quarry operations, *Transactions of the American Institute of Mining, Metallurgical Petroleum Engineers*, Vol. 220, pp. 271-274, 1961.

[5] BALASUBRAMANIAN, A.: Size reduction by crushing methods, ResearchGate, pp. 1-10, 2017. https://doi.org/10.13140/RG.2.2.28195.45606

[6] SAPIETOVÁ, A., DEKÝŠ, V.: Dynamic analysis of rotating machines in MSC ADAMS, *Procedia Engineering*, Vol. 136, pp. 143-149, 2016.

[7] BOCKO, J., DELYOVÁ, I., FRANKOVSKÝ, P.: *Kinematik*a, Košice, 2012. (Original in Slovak)

[8] DELYOVÁ, I., HRONCOVÁ, D., FRANKOVSKÝ, P.: Analysis of simple mechanism using MSC Adams, *Manufacturing Technology*, Vol. 14, No. 2, pp. 141-145, 2014.

[9] HRONCOVÁ, D., DELYOVÁ, I.: Computer Simulation Using MSC ADAMS, *Acta Mechatronica*, Vol. 5, No. 3, pp. 41-46, 2020. https://doi.org/10.22306/am.v5i3.67

[10] SAPIETOVÁ, A., SÁGA, M., KURIC, I., VÁCLAV, Š.: Application of optimization algorithms for robot systems designing, *International journal of advanced robotic systems*, Vol. 15, No. 1, 2018.

[11] MAHMOOD, K., ISMAIL, N.A.: Application of multibody simulation tool for dynamical analysis of tethered aerostat, *Journal of King Saud University-Engineering Sciences*, Vol. 34, No. 3, pp. 209-216, 2020.

[12] ARMAN, R.: *Kinematic analysis on four-bar mechanism model using PID Controller*, The 5th Engineering Science & Technology International Conference, IOP Publishing, IOP Conf. Series: Materials Science and Engineering 990, 2020. 10.1088/1757-899X/990/1/012029

[13] HRONCOVÁ, D., FRANKOVSKÝ, P., VIRGALA, I., DELYOVÁ, I.: Kinematic Analysis of the Press Mechanism Using MSC Adams, *American journal of mechanical engineering*, Vol. 2, pp. 312-315, 2014.

[14] ZAR, T., LIN, P.W., WIN, S.Y.: Workspace Analysis of Two-link Planar Manipulator, *Int. J. of Science and Engineering Applications*, Vol. 8, pp. 380-383, 2019.

Review process

Single-blind peer review process.

doi:10.22306/am.v7i1.84

Received: 05 Feb. 2022
Revised: 17 Feb. 2022
Accepted: 07 Mar. 2022

Pick & Place automated workplace based on CC-Link IE Field basic communication

Jaroslav Romancik
Technical University of Kosice, Faculty of Mechanical Engineering, Letna 1/9, Kosice, Slovak Republic, EU, jaroslav.romancik@tuke.sk (corresponding author)
Marek Vagas
Technical University of Kosice, Faculty of Mechanical Engineering, Letna 1/9, Kosice, Slovak Republic, EU, marek.vagas@tuke.sk
Alena Galajdova
Technical University of Kosice, Faculty of Mechanical Engineering, Letna 1/9, Kosice, Slovak Republic, EU, alena.galajdova@tuke.sk

Keywords: collaborative robot, PLC, camera sensor, communication.
Abstract: The article offers a proposal for communication between the collaborative robotic system and the PLC control concerning the CC-LINK IE FIELD BASIC communication protocol. The solution tests the principle of "*Master*" and "*Slave*," where the preferred system is the PLC (from the product company Mitsubishi). In general, there are many possibilities for communication, so this article orients toward Ethernet-type communication. It also includes an innovative interconnection of the components of the different manufacturers (Mitsubishi, VENGLOR, and others) and verification on a real application example of the type "*Pick & Place*."

1 Introduction

At present, collaborative robotics is on the rise. Its deployment is constantly being extended to the already run automated process to reduce costs or the need to implement complex additional safety devices (such as a safety cage, a firewall, etc.). The collaborative robot provides a sufficiently high safety standard for a human operator near (or part of) the running process. In many cases, however, the automated process requires using existing peripheral devices, and thus the communication solution becomes more important [1]. Communication between the robot system and other peripherals (camera, sensors, security features) is necessary for the correct and complete operation of the automated process. The ideal solution, especially in the "Pick & Place" cases, is to install a specific version of the recognition system, e.g., a 2D camera sensor.

Visual systems have an invaluable impact on automation processes and are crucial to their variable use for their many implemented functions and programming capabilities. Applications are found in processes where rapid diagnosis and evaluation of the scanned image are required. The most used parts of the visual systems are the assessment of the quality of the object and the correct dimension [2]. It may lead to a significant increase in the rate of production and control of the products produced. In conjunction with robotic devices, their application increases, particularly when determining the coordinates of scanned objects in cases where it is impossible to precisely define their position. However, to ensure the automated process's correct functionality and the application solution's smooth operation, it is advantageous (and almost always necessary) for raw data collected from the visual system to be modified (aggregation). The ideal device to adjust is the PLC system. In such a case, it plays the role of an "intermediary" and performs the function of a superior system in the visual sensor hierarchy and robotic equipment [3]. Plc not only receives these data from the optical sensor but also sorts them and edits them into the correct data type, according to the camera type and the robotic device control unit, Figure 1.

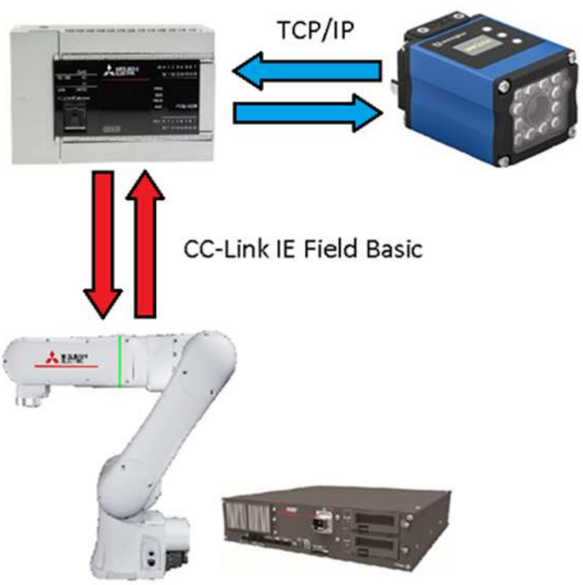

Figure 1 Flow of communication data between the various devices of an automated workstation

Acta Mechatronica - International Scientific Journal about Mechatronics
Volume: 7 2022 Issue: 1 Pages: 9-12 ISSN 2453-7306

2 Hardware components

To ensure the proposed and functional cooperation in an automated workplace, we use a camera sensor (from WENGLOR), a PLC system FX5U (from MITSUBISHI), and a collaborative robot (MELFA ASSISTA, also from MITSUBISHI).

Specifically, the selected camera sensor has several tools to assist and refine the detection result. This device combines a color scanner and visual sensor functions. As a result, it can scan objects of different colors, recognize their shape, and scan and read 1D and 2D codes. In addition, it includes an automatic focus function or object tracking according to the projected pattern. It can also count objects, measure their size, and determine their position [4].

MELFA ASSISTA is a vertical 6-axis collaborative robot with a maximum range of 910 mm, a payload of 5 kg, and repeatability of the position of ± 0.03 mm [5]. It can operate in three basic speed modes, namely:

- Collaborative mode slow (up to 50 mm / s).
- Collaborative standard mode (up to 250 mm / s).
- High-speed mode (up to 1000 mm / s).

An FX5U-type PLC is a compact PLC. Therefore, it is suitable for smaller applications. It is equipped with high-speed 16 digital inputs (24VDC), 16 outputs (relays/transistors), two analog inputs, and one analog output [6]. It also contains a standard error monitoring, LED status indication, or SD card slot. Its most significant advantage is its low price and its small size. The use options are mostly fixed, but thanks to extensions, it offers a degree of variability. The most used extensions are expansion modules to expand inputs and outputs or memory extensions.

3 Communication principle

The basic principle of the proposed communication between the individual Pick & Place workstations is the TCP / IP-based communication protocol, Figure 2. The PLC device (as a preferred system) opens a communication channel and allows the necessary data to be exchanged between the two parties (Master and Slave). The camera sensor retrieved from the inspection sends the information directly to the pre-configured PLC communication port of the device, which is specifically assigned for this type of communication. After a successful data transmission, the communication channel is closed.

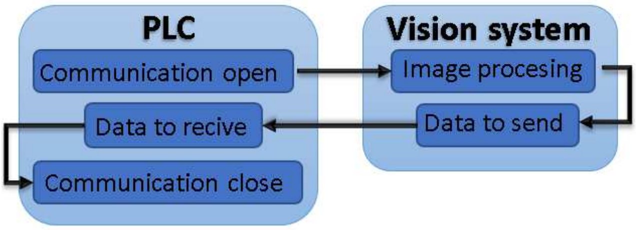

Figure 2 Principle of TCP / IP protocol communication

If we want to understand the principle of communication, it is necessary to explain the CC-Link IE Field Basic communication protocol. CC-Link IE Field Network Basic is a part of CC-Link IE Network and realizes easier network connection of Ethernet devices. Banner communications are achieved by utilizing SLMP, which enables seamless connectivity within all levels of manufacturing [7]. It is a communication protocol that serves specifically and exclusively used for MITSUBISHI facilities. The necessary condition for this communication protocol's setting (opening) is its authorization by the robotic system. The transmission and reception of data by the PLC of the device are secured by defining the bit field length for receiving and transmitting data (Bool type). By analogy, data fields for receiving and sending data in the corresponding (WORD type) are also reserved.

Link Side					CPU Side				
Device Name	Points	Start	End		Target	Device Name	Points	Start	End
RX	64	00000	0003F	⇔	Specif	B	64	00000	0003F
RY	64	00000	0003F	⇔	Specif	B	64	00070	000AF
RWr	32	00000	0001F	⇔	Specif	W	32	00000	0001F
RWw	32	00000	0001F	⇔	Specif	W	32	00040	0005F

Figure 3 Range settings for the data fields for the CC-Link IE Field Basic communication protocol

Adjustment (Figure 3) means that the data stored in the PLC storage area (whether of the Bool type or WORD type) correspond to an associated address on the robotic device side (corresponding to 6000 addresses for inputs and outputs in the case of robotic devices from MITSUBISHI).

4 Object detection

Adjustment (Figure 3) means that the data stored in the PLC storage area (whether of the Bool type or WORD type) correspond to an associated address on the robotic device side (corresponding to 6000 addresses for inputs

Acta Mechatronica - International Scientific Journal about Mechatronics
Volume: 7 2022 Issue: 1 Pages: 9-12 ISSN 2453-7306

and outputs in the case of robotic devices from MITSUBISHI).

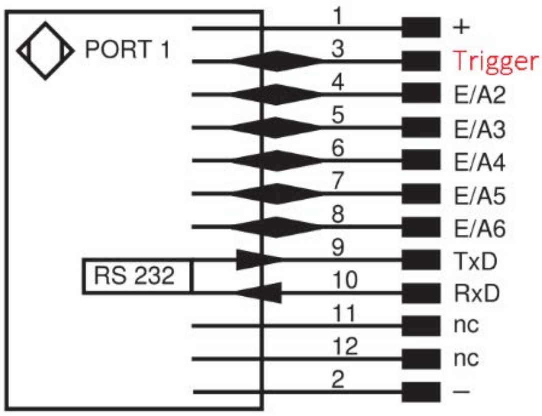

Figure 1 Trigger pin for objects' picture capturing

The PLC device also sends a color change signal to the 2D camera sensor. Since the 2D camera sensor program cannot work with the branch, changing the desired color is achieved by changing the entire 2D camera sensor program by sending a specific signal to the specified output. From the point of view of the use of functionalities, the "*Threshold*" function is an excellent tool. It is a function that filters the color of pixels based on a pre-set filter. Compliant pixels are white, while non-compliant pixels are black, figure 5.

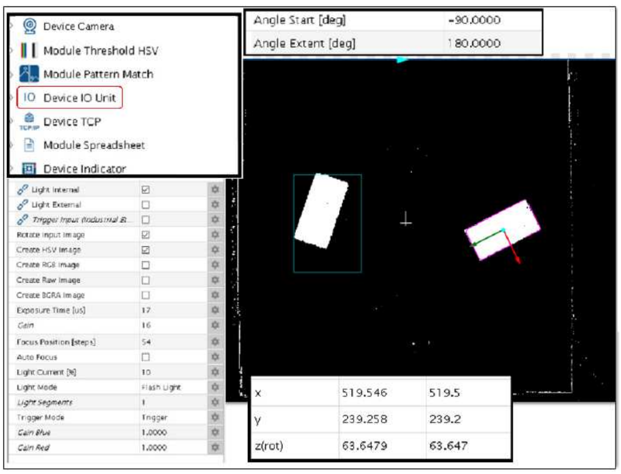

Figure 2 Example of "Threshold" function usage

Another excellent and frequently used functionality is the "pattern match" function. It will be used mainly in detection processes where the shape and size of the object sought are known in advance. The principle of the above procedure is to search for objects that correspond to the set stored (database) pattern. Then, if a match is made and the system finds several compliant objects, the one with the highest percentage match with the pre-set way shall be automatically selected.

At the same time, the function allows the coordinates (x, y) and the rotation of the detected object with the highest percentage of agreement with the pattern to be determined. This information is key to guiding the robotic system into the correct position to grasp the desired object.

5 Application testing

The main task of the "Pick & Place" experimental solution of the automated workstation is to create an application that would sufficiently and effectively test the communication process between the various facilities involved. The application's functionality is based on a camera vision, by which an object is subsequently found in the view field of the 2D camera sensor, Figure 6.

This object's coordinates are subsequently transmitted to the robot (collaborative robot control system) using the PLC device. The robot, thanks to the information received on the position of the object, performs a grasping action on the object. Then is correctly classified according to the attributes defined in the front (e.g., in the corresponding suspending box).

Figure 3 Layout of the automated workplace

The automated process presupposes that the robot system is set to the reference position (depending on the coordinates of the object being sought). The coordinates found are then transmitted in the form of the data type "String" to the PLC device. It is solved by the TCP / IP communication protocol. In the next steps of the PLC, the device processes, adjust and compiles the information obtained so that the information about the coordinates of the object can be understood and correctly read by the robot system. The final step is the movement of the collaborative robotic arm according to the coordinates obtained, grasping the object sought and moving above the stop position where the process ends.

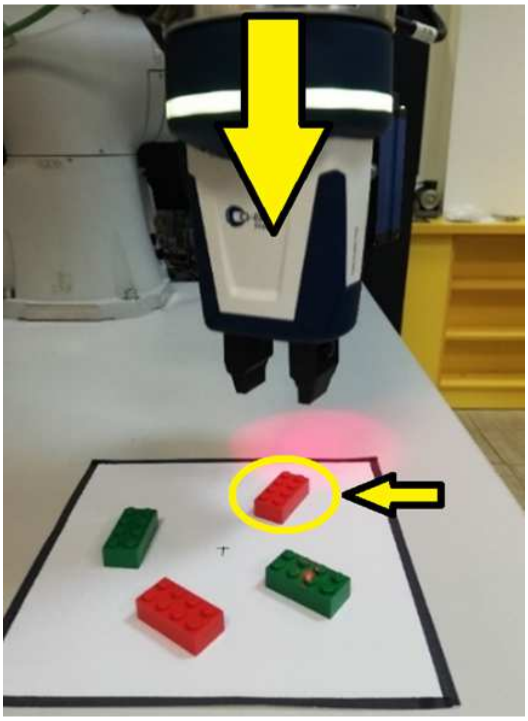

Figure 4 Pick & Place position for a founded object

6 Conclusion

Camera systems are now an essential part of automated workplaces, where the participation of robotic arms is indispensable. Therefore, the solution of the topology for communication, communication protocols, and the nature of the processing (aggregation) of the data offer scope for experimentation, testing, and subsequent verification of the proposed solutions (such as this). Furthermore, they will find their use in the quality control of products and their dimensions and in advanced systems for managing complex automation processes.

Thanks to such application examples, the need to use additional staff for the manual and lengthy work that such a solution offer is no longer needed.

Acknowledgment
This work has been supported by the Slovak Grant KEGA 044TUKE-4/2021-Remote access to laboratory exercises for industrial automation and Slovak Grant VEGA 1/0169/22 New methodics approaches to data from automated and robotized workplaces.

References

[1] VARGA, M., VAGAŠ, M.: Experimental vision system setup based on the serial configuration interface, *Acta Mechatronica*, Vol. 6, No. 3, pp. 41-44, 2021. https://doi.org/10.22306/am.v6i3.77
[2] VAGAŠ, M., ŠEMINSKÝ, J.: Approaches for the 3D camera system image processing at automated workplaces, *Technical Sciences and Technologies, Chernihiv*, Vol. 22, No. 4, pp. 150-155, 2020.
[3] KURYŁO, P., FRANKOVSKÝ, P., PAPACZ, W., DELYOVÁ, I., SCHURGER, B.: Design of an automated system for measuring car bodies, *Acta Mechatronica*, Vol. 6, No. 1, pp. 11-20, 2021. https://doi.org/10.22306/am.v6i1.74
[4] VIRGALA, I., MIKOVÁ, Ľ., SUKOP, M., VAGAŠ, M, LIPTÁK, T., KELEMEN, M.: *Sensors and transducers*, *Snímače a prevodníky*, Kosice, TU, 2017.
[5] SEMJON, J., JANOS, R., SUKOP, M., TULEJA, P., HAJDUK, M., JURUS, O., MARCINKO, P., VIRGALA, I., VAGAS, M.: Verification of the UR5 robot's properties after a crash caused by a fall of a transferred load from a crane, *International Journal of Advanced Robotic Systems*, Vol. 17, No. 1, pp. 1-9, 2020. https://doi.org/10.1177/1729881420904209
[6] VAGAŠ, M., GALAJDOVÁ, A., ŠIMŠÍK, D., ONOFREJOVÁ, D.: *Wireless data acquisition from automated workplaces based on RFID technology*, IFAC-PapersOnLine, Vol. 52, No. 27, pp. 299-304, 2019. https://doi.org/10.1016/j.ifacol.2019.12.677
[7] RÁKAY, R., GALAJDOVÁ, A., ŠEMINSKÝ, J., CVITIĆ, I.: Selected wireless communication protocols and their properties for use in IoT systems, *Research papers Faculty of Materials Science and Technology in Trnava, Slovak University of Technology in Bratislava*, Vol. 27, No. 45, pp. 26-32, 2019. https://doi.org/10.2478/rput-2019-0022

Review process
Single-blind peer review process.

JOURNAL STATEMENT

Journal name:	**Acta Mechatronica**
Abbreviated key title:	Acta Mechatron
Journal title initials:	AM
Journal doi:	10.22306/am
ISSN:	2453-7306
Start year:	2016
The first publishing:	March 2016
Issue publishing:	Quarterly
Publishing form:	On-line electronic publishing
Availability of articles:	Open Access Journal
Journal license:	CC BY-NC
Publication ethics:	COPE, ELSEVIER Publishing Ethics
Plagiarism check:	Worldwide originality control system
Peer review process:	Single-blind review at least two reviewers
Language:	English
Journal e-mail:	**info@actamechatronica.eu**

The journal focuses mainly on original, interesting, new and quality, theoretical, practical and application-oriented contributions to the scientific fields and research as well as to pedagogy and training in mechatronics.

Publisher:	**4S go, s.r.o.**
Address:	Semsa 24, 044 21 Semsa, Slovak Republic, EU
Phone:	+421 948 366 110
Publisher e-mail:	**info@4sgo.eu**

Responsibility for the content of a manuscript rests upon the authors and not upon the editors or the publisher.